

# Approximations in Fusion and Breakup reactions induced by Radioactive Beams

W.H.Z. Cárdenas<sup>1</sup>, L.F. Canto<sup>2</sup>, R. Donangelo<sup>2</sup>, M.S. Hussein<sup>1</sup>, J. Lubian<sup>3</sup> and A. Romanelli<sup>4</sup>

<sup>1</sup>*Instituto de Física, Universidade de São Paulo,  
C.P. 66318, 05389-970 São Paulo, Brazil*

<sup>2</sup>*Instituto de Física, Universidade Federal do Rio de Janeiro,  
C.P. 68528, 21945-970 Rio de Janeiro, Brazil,*

<sup>3</sup>*Instituto de Física, Universidade Federal Fluminense,  
Av. Litorânea S-N, 24210-340 Niteroi, Rio de Janeiro, Brasil*

*and*

*CEADEN, Havana, Cuba*

<sup>4</sup>*Instituto de Física, Facultad de Ingeniería,  
C.C. 30, Montevideo, Uruguay*

(October 27, 2018)

## Abstract

Some commonly used approximations for complete fusion and breakup transmission coefficients in collisions of weakly bound projectiles at near barrier energies are assessed. We show that they strongly depend on the adopted classical trajectory and can be significantly improved with proper treatment of the incident and emergent currents in the WKB approximation.

## I. INTRODUCTION

In a fusion reaction the projectile and target nuclei form an excited compound system, which decays by emission of particles or gamma rays. When there are channels strongly coupled to the elastic channel, the reaction may be described using any of the available coupled channels codes. The effects of such couplings have been extensively discussed in the literature [1]. In general terms, at energies below that of the Coulomb barrier, these couplings tend to reduce the effective fusion barrier, which substantially increases the fusion cross section. At high energies the incident flux in the elastic channel is partially diverted into inelastic and transfer channels. This tends to decrease the contribution of the elastic channel to the fusion cross section, but this reduction is partially compensated by the contribution from the other channels.

The recent availability of radioactive beams has made possible to study reactions involving unstable nuclei. Such reactions are important in processes of astrophysical interest, as well as in the search for superheavy elements. The main new ingredient in reactions induced by unstable projectiles is the strong influence of the breakup channel. In the case of not too unstable projectiles, the effect of this channel in the fusion cross section at low energies is, as in the case of stable beams, to enhance it. At high energies, however, the situation is qualitatively different from the case where only stable nuclei are involved. The contribution from the breakup channel to the fusion reaction is strongly influenced by the low probability that all fragments are captured. Thus, in this case, the fusion cross section is partitioned into a complete and one or more incomplete fusion contributions [2].

The introduction of the breakup channel into a coupled channels calculation is by no means trivial. The difficulty lies in the fact that this channel lies in the continuum, and involves a, at least, three body system. This problem has been addressed by several authors, using different approaches. Several recent experiments involving fusion of neutron rich  ${}^6\text{He}$  and proton rich  ${}^{17}\text{F}$  with heavy targets have been performed with the purpose of exploring these theoretical proposals [3–5]. In Refs. [2,6–9], the coupled-channel problem is simplified by the introduction of the polarization potentials arising from the coupling with the breakup channel [10,11]. In Refs. [12–14], the coupled-channel problem is solved directly within different approximation, ranging from the schematic model of Dasso and Vituri [12] to the huge calculation of Hagino *et al.* [14], performed through continuum discretization.

The polarization potential approach of Refs. [2,6–9] has the advantage of leading to simple expressions, which can easily be used in data analysis [15]. However, it employs several approximations which were not thoroughly tested. These approximations can be grouped in two categories. In the first are those used in the derivation of the polarization potentials. In the second are the semiclassical approximations for fusion and breakup coefficients, used in calculations of the cross sections. These coefficients are written in terms of barrier penetration factors and survival probabilities, which are evaluated within the WKB approximation. The aim of the present work is to ascertain the quality of the approximations for the transmission coefficients. Approximations in the derivation of the polarization potential will be the object of a latter study. For our purposes, we consider a case where a complete quantum mechanical calculation is feasible and compare exact and approximated cross sections. We study the  ${}^{11}\text{Li} + {}^{12}\text{C}$  collision, using typical optical and polarization potentials. For simplicity, our polarization potential has no angular momentum or energy dependence

and the range is given by the  $^{11}\text{Li}$  breakup threshold energy. The strength is consistent with that found in Ref. [10] for the most relevant partial waves in near-barrier fusion.

The plan for this paper is as follows: in section II we briefly revise the coupled channels formalism and the concept of a polarization potential. In section III we discuss different approximation for the transmission coefficients and investigate their consequences on the fusion and breakup cross sections. Finally, in section IV, we present the conclusions of this work.

## II. COUPLED CHANNEL EQUATIONS AND POLARIZATION POTENTIALS

In a standard coupled channels calculation, the system is described through the distance between centers of projectile and target,  $\mathbf{r}$ , and a set of intrinsic coordinates,  $\xi$ , that describe the internal degrees of freedom of one of the nuclei, *e.g.* the target. These coordinates are associated to an intrinsic Hamiltonian  $h$  and its eigenfunction set,

$$h\phi_\alpha(\xi) = \epsilon_\alpha\phi_\alpha(\xi), \quad (1)$$

where

$$\int \phi_\alpha^*(\xi)\phi_\beta(\xi)d\xi = \delta_{\alpha,\beta}. \quad (2)$$

The system Hamiltonian may then be written as

$$H = T + U^{opt} + h + v(\mathbf{r}, \xi). \quad (3)$$

Above,  $T$  is the kinetic energy of the relative motion,  $U^{opt}$  is the optical potential and  $v(\mathbf{r}, \xi)$  is the interaction coupling intrinsic and collision degrees of freedom. The optical potential, which is diagonal in channel space, accounts for the average interaction between projectile and target.

Usually the solution of Schrödinger's equation

$$H\Psi(\mathbf{r}, \xi) = E\Psi(\mathbf{r}, \xi), \quad (4)$$

where  $E$  is the collision energy in the center of mass frame, is expanded as

$$\Psi(\mathbf{r}, \xi) = \sum_{\alpha} \psi_{\alpha}(\mathbf{r})\phi_{\alpha}(\xi), \quad (5)$$

where  $\psi_{\alpha}(\mathbf{r})$  describes the relative motion in channel  $\alpha$ . Substituting this expansion in Eq. (4) we obtain the coupled channels equations (see *e.g.* Ref. [16]),

$$(E_{\alpha} - H_{\alpha})\psi_{\alpha}(\mathbf{r}) = \sum_{\beta} \mathcal{V}_{\alpha\beta}(\mathbf{r})\psi_{\beta}(\mathbf{r}). \quad (6)$$

Above,  $E_{\alpha} = E - \epsilon_{\alpha}$  and  $H_{\alpha} = T + U_{\alpha}^{opt}(r)$ , where

$$U_{\alpha}^{opt} \equiv V_{\alpha}^{opt} - i W_{\alpha}^{opt} \quad (7)$$

is the optical potential in channel  $\alpha$ . The imaginary parts have the purpose of accounting for the flux lost to channels neglected in the expansion of Eq.(5). The channel coupling potentials, in Eq.(6) are given by

$$\mathcal{V}_{\alpha\beta}(\mathbf{r}) = \int d\xi \phi_{\alpha}^*(\xi) v(\mathbf{r}, \xi) \phi_{\beta}(\xi). \quad (8)$$

A consequence of the non-Hermitian nature of  $H$  (see Eq.(7)) is that the continuity equation breaks down. This can be checked following the usual procedure to derive the continuity equation. For each  $\alpha$ , we evaluate  $\psi_{\alpha}^*(\mathbf{r}) \times [\text{Eq.}(6)] - [\text{Eq.}(6)]^* \times \psi_{\alpha}(\mathbf{r})$  and then sum the results. Assuming that  $\mathcal{V}_{\alpha\beta}$  is hermitian, we obtain

$$\nabla \cdot \sum_{\alpha} \mathbf{j}_{\alpha} = \frac{2}{\hbar} \sum_{\alpha} W_{\alpha}^{opt}(\mathbf{r}) |\psi_{\alpha}(\mathbf{r})|^2 \neq 0$$

Integrating the above equation inside a large sphere with radius larger than the interaction range and using the definition of the absorption cross section, we obtain the useful relation [17]

$$\sigma_a = \frac{k}{E} \sum_{\alpha} \langle \psi_{\alpha} | W_{\alpha} | \psi_{\alpha} \rangle. \quad (9)$$

### A. Polarization potentials

In some coupled channel problems, it occurs that one is only interested in the elastic wave function. One example is the study of complete fusion in collisions involving nuclei far from stability, where the breakup threshold is very low. An extreme example is  $^{11}\text{Li}$ , which has no bound excited state. In such cases, the coupled channel problem involves only the elastic and the breakup channels. Since the breakup channels contain at least three fragments, their contribution to complete fusion is expected to be negligible. Therefore, only the elastic wave function is required for the calculation of the complete fusion and breakup cross sections.

In such cases, the *polarization potential* approach becomes very convenient. It consists of replacing the coupled channel equations by a single Schrödinger equation for the elastic state. This equation contains a *polarization* term,  $U^{pol}$ , added to the optical potential and its solution is identical to the elastic wave function obtained from the coupled channel equations. According to Feshbach [18], the polarization potential is obtained through elimination of the coupled channel equations for excited states and it is given by

$$U^{pol} = (\phi_0 | P v Q G_{QQ}^{(+)} Q v P | \phi_0). \quad (10)$$

Above,  $P = |\phi_0\rangle\langle\phi_0|$  is the projector on the elastic channel,  $Q = 1 - P = \sum_{\alpha \neq 0} |\phi_{\alpha}\rangle\langle\phi_{\alpha}|$ , and the propagator  $G_{QQ}^{(+)}$  is defined as

$$G_{QQ}^{(+)} = \frac{1}{E - Q H_0 Q + i\epsilon}. \quad (11)$$

The wave function is then obtained by solving

$$(E - H_0 - U^{pol})|\psi_0\rangle = 0, \quad (12)$$

which, in the position representation is written

$$\left[ E - T - U^{opt}(\mathbf{r}) \right] \psi(\mathbf{r}) - \int U^{pol}(\mathbf{r}, \mathbf{r}') \psi(\mathbf{r}') d^3\mathbf{r}' = 0, \quad (13)$$

where  $U^{pol}(\mathbf{r}, \mathbf{r}')$  is the nonlocal potential

$$U^{pol}(\mathbf{r}, \mathbf{r}') = \sum_{\alpha} V_{0\alpha}(\mathbf{r}) G^{(+)}(E_{\alpha}; \mathbf{r}, \mathbf{r}') V_{\alpha 0}(\mathbf{r}'). \quad (14)$$

In principle, evaluating the polarization potential is nearly as hard as solving the coupled channel equations. However, for practical purposes it is replaced by trivially equivalent local potentials, which are calculated with approximations [10,11].

## B. Fusion and breakup cross sections

With the introduction of the polarization potential, any flux going away from the elastic channel is treated as absorption. The sum in Eq. (9) is then reduced to a single term, the one with  $\alpha = 0$ . The imaginary part of the potential is (henceforth we drop the superfluous index  $\alpha$ , since only the elastic channel appears),

$$W = W^{opt} + W^{pol}, \quad (15)$$

the absorption cross section can be split as

$$\sigma_a = \sigma_F + \sigma_{bu}. \quad (16)$$

Above,

$$\sigma_F = \frac{k}{E} \int d^3\mathbf{r} W^{opt}(r) |\psi(\mathbf{r})|^2 \quad (17)$$

is identified with absorption through complete fusion and

$$\sigma_{bu} = \frac{k}{E} \int d^3\mathbf{r} W^{pol}(r) |\psi(\mathbf{r})|^2 \quad (18)$$

corresponds to the loss of flux through the breakup channel. It includes the breakup cross section and also a cross section for absorption in the breakup channels, probably incomplete fusion. However, since for weakly bound nuclei the range of  $W^{pol}$  is much larger than that of  $W^{opt}$ , we neglect this contribution and use the notation  $\sigma_{bu}$  in Eq. (18).

It is useful to consider the expansion in partial waves of the wavefunction,

$$\psi = \sum_{l,m} \frac{u_l(k, r)}{r} Y_{lm}(\theta, \varphi), \quad (19)$$

where  $k = \sqrt{2\mu E/\hbar^2}$  and the  $u_l(k, r)$  are solutions of the radial equation,

$$-\frac{\hbar^2}{2\mu} \left[ \frac{d^2}{dr^2} - \frac{l(l+1)}{r^2} \right] u_l(k, r) + U^{opt}(r) u_l(k, r) = E u_l(k, r), \quad (20)$$

normalized such that

$$u_l(k, r \rightarrow \infty) = \frac{i}{2} \left[ H_l^{(-)}(kr) - S_l H_l^{(+)}(kr) \right]. \quad (21)$$

Using the partial wave expansion in Eq.(17), the fusion cross section may be rewritten as

$$\sigma_F = \frac{\pi}{k^2} \sum_l (2l+1) T_l^F, \quad (22)$$

where the transmission coefficient is given by

$$T_l^F = 1 - |S_l|^2 = \frac{4k}{E} \int_0^\infty dr W^{opt}(r) |u_l(k, r)|^2. \quad (23)$$

Proceeding similarly with Eq.(18), we get

$$\sigma_{bu} = \frac{\pi}{k^2} \sum_l (2l+1) T_l^{bu}, \quad (24)$$

with

$$T_l^{bu} = \frac{4k}{E} \int_0^\infty dr W^{pol}(r) |u_l(k, r)|^2. \quad (25)$$

### III. APPROXIMATIONS

In what follows, we study different approximations to the coefficients  $T_l^F$  and  $T_l^{bu}$ . In order to fix ideas, we consider a  $^{11}\text{Li}$  beam incident on a  $^{12}\text{C}$  target, using an optical potential  $U^{opt} = V^{opt} - i W^{opt}$  parameterized in the standard way:

$$V^{opt}(r) = V^N(r) + V^C(r), \quad (26)$$

with the nuclear part given by

$$V^N(r) = \frac{V_0^N}{1 + \exp[(r - R_r)/a_r]}, \quad (27)$$

and the Coulomb one by

$$\begin{aligned} V^C(r) &= Z_p Z_t e^2 / r; & \text{for } r > R_C \\ &= (Z_p Z_t e^2 / 2R_C) \left[ 3 - \left( \frac{r}{R_C} \right) \right]^2; & \text{for } r \leq R_C. \end{aligned} \quad (28)$$

Above,  $Z_p, A_p$  ( $Z_t, A_t$ ) are the atomic and mass numbers of the projectile (target),  $R_C$  is the radius of the nuclear charge distribution, and  $R_r$  is given by

$$R_r = r_r^0 \left( A_p^{1/3} + A_t^{1/3} \right). \quad (29)$$

The imaginary part is similarly parameterized as

$$W^{opt}(r) = \frac{W_0^{opt}}{1 + \exp[(r - R_i)/a_i]}, \quad (30)$$

with  $R_i$  defined similarly to Eq.(29). We take the following parameter values:

$$V_0^{opt} = -60 \text{ MeV}; \quad r_r^0 = 1.25 \text{ fm}; \quad a_r^0 = 0.60 \text{ fm}; \quad (31)$$

$$W_0^{opt} = 60 \text{ MeV}; \quad r_i^0 = 1.00 \text{ fm}; \quad a_i^0 = 0.60 \text{ fm}. \quad (32)$$

Note that, since  $W^{opt}$  corresponds exclusively to short range fusion absorption,  $r_i^0$  is appreciably smaller than  $r_r^0$ .

In order to review the standard approximations in the optical potential calculations, we initially disconsider the breakup channels. In the absence of breakup, the imaginary part of the nuclear potential has a short range, and therefore fusion may be approximately described through an infinitely absorbing imaginary potential with a well defined radius  $R_F$ . In this case  $T_l^F$  may be estimated by  $T_l$ , the transmission coefficient through the effective potential

$$V_l(r) = V^{opt}(r) + \frac{\hbar^2 l(l+1)}{2\mu r^2}. \quad (33)$$

If one approximates the region around the maximum of  $V_l$  by a parabola, then one obtains the Hill-Wheeler expression for  $T_l^F$  [19]

$$T_l^F \approx T_l \approx T_l^{HW} = \left\{ 1 + \exp \left[ 2\pi \left( \frac{B_l - E}{\hbar\omega_l} \right) \right] \right\}^{-1}, \quad (34)$$

where  $R_B$  is the position of this maximum,  $B_l$  its value, and  $\omega_l$  the curvature of  $V_l$  at  $r = R_B$ ,

$$\hbar\omega_l = \left( - \frac{\hbar^2}{\mu} \left[ \frac{d^2 V_l(r)}{dr^2} \right]_{R_B} \right)^{1/2}. \quad (35)$$

In Fig. 1, we show an example of a cross section calculated within the Hill-Wheeler approximation (dashed line) compared with the exact quantum mechanical calculation (full circles). One notices that the approximation is excellent at energies above the Coulomb barrier,  $E > V_B \equiv B_{l=0}$ , but worsens rapidly for  $E \ll V_B$ .

The problem at low energies may be improved using the WKB approximation. The transmission factor is then given by

$$T_l \approx \exp(-2\Phi) \quad (36)$$

where

$$\Phi = \text{Im} \left\{ \int_{r_{in}}^{r_{out}} k(r) dr \right\}. \quad (37)$$

Above,

$$k(r) = \frac{1}{\hbar} \sqrt{2\mu [E - V_l(r)]} \quad (38)$$

and  $r_{in}$  e  $r_{out}$  are the inner and outer classical turning points for the potential  $V_l$ , determined through the condition  $V_l(r_{in(out)}) = E$ . However, this approximation is not good at energies  $E \approx B_l$ ; for  $E = B_l$  it yields  $T_l = 1$  instead of the correct value  $T_l = 1/2$ , and even worse, it does not predict reflections above the barrier. Improvement is obtained by substituting the approximation of Eq. (36) by Kemple's expression [20] below the barrier while keeping Hill-Wheeler's approximation above it,

$$T_l = (1 + e^{2\Phi})^{-1} (E < B_l); \quad T_l = T_l^{HW} (E \geq B_l). \quad (39)$$

We have employed this approximation in Ref. [2]; it is equivalent to employing the Hill-Wheeler formula for all energies, albeit with the modification

$$\frac{\pi}{\hbar\omega_l}(B_l - E) \longrightarrow \Phi; \quad \text{for } E > B_l.$$

The cross section obtained within this approximation is depicted in Fig. 1 (solid line). We see that it reproduces the full quantum calculations for all collision energies.

Let us now consider the inclusion of the breakup channels. As we have seen, this may be done through the introduction of an appropriate polarization potential. Such potentials were studied in Refs. [7,8], for pure nuclear coupling, and in [9,11] for the electromagnetic coupling. In [7,8] only the imaginary part of the polarization potential was calculated. Since the real part of the polarization potential reduces the height of the potential barrier, this effect was simulated by a shift in the collision energy in the calculation of  $T_l$ . Namely,

$$T_l(E) \rightarrow T_l(E + \Delta E); \quad \Delta E = -V^{pol}(R_B).$$

As we will see, the real part of the polarization potential plays a very important role at energies below the Coulomb barrier. In the case of  $^{11}\text{Li} + ^{12}\text{C}$ , the breakup process is dominated by the nuclear coupling. Therefore we write

$$W^{pol}(r) = \frac{W_0^{pol}(l, E_{CM})}{1 + \exp[(r - R_{pol})/\alpha]}, \quad (40)$$

where  $R_{pol}$  may be approximated by the optical potential radius, and the diffuseness  $\alpha$  is given in terms of the breakup threshold energy  $B_{bu}$  as

$$\alpha = \left( \frac{2\mu_{bu} B_{bu}}{\hbar^2} \right)^{1/2}. \quad (41)$$

Above,  $\mu_{bu}$  is the reduced mass of the fragments produced in the breakup process. In the case of  $^{11}\text{Li}$ ,  $B_{bu} = 0.2$  MeV and thus  $\alpha = 6.6$  fm.



The strength of the polarization potential varies with  $l$  and  $E_{CM}$ , and, for the partial waves relevant to the fusion process, is of the order of 1 MeV in the region around  $r \approx R_{pol}$ . Since in this work we are not concerned with its derivation, but with the approximations employed in the determination of the cross section, we shall adopt the constant value

$$W_0^{pol}(l, E) \equiv W_0^{pol} = 2.0 \text{ MeV} . \quad (42)$$

Since the real part of the polarization plays a very important role at energies below the Coulomb barrier, we shall include it here. In the calculations of Andrés *et al.* [11] the real and imaginary parts of the polarization potential have qualitatively the same strengths. For simplicity we then take them to be equal, *i.e.*

$$V_0^{pol}(l, E) \equiv V_0^{pol} = -2.0 \text{ MeV} . \quad (43)$$

The effect of the real and imaginary parts of the polarization potential are shown in Fig. 2. As it could be expected, the real part leads to a substantial increase in the fusion cross section, most evident at energies below the Coulomb barrier. On the other hand, the imaginary part reduces the cross section both above and below the barrier. When both the real and imaginary parts are included, there is a competition between the effects of the real and imaginary parts. With the polarization strength values considered above, suppression dominates above the barrier and enhancement below it. This situation was also encountered in the coupled channels calculations of Breitschaft *et al.* [13] and Hagino *et al.* [14].

The presence of a long-ranged absorption requires the introduction of modifications in the approximations to  $T_l^F$ . Now the flux that reaches the strong absorption region is attenuated not only because of the reflection at the barrier, but also because of its absorption into the breakup channel. In Ref. [6] it was proposed the approximation

$$T_l^F \approx T_l(E + \Delta E) \cdot P_l^{surv} , \quad (44)$$

where  $T_l(E + \Delta E)$  is the WKB transmission factor (Eq. (36)) evaluated at the energy  $E + \Delta E$  and  $P_l^{surv}$  is the breakup survival probability. Within the WKB approximation we may take

$$P_l^{surv} = \exp \left[ -\frac{2}{\hbar} \int \frac{W^{pol}(r)}{v_l(r)} dr \right] , \quad (45)$$

where  $v_l(r)$  is the local radial velocity along a classical trajectory with angular momentum  $\hbar l$ . A more formal justification for Eq (44), based on a WKB calculation with three turning points was presented in Ref. [8]. This approximation is consistent with the results of Fig. 2. The enhancement due to  $V^{pol}$  is included in  $T_l$  while the suppression arising from  $W^{pol}$  is contained in  $P_l^{surv}$ .

In order to estimate  $P_l^{surv}$  one needs to define the classical trajectories to be employed in the calculation. In Ref. [6] we considered pure Rutherford trajectories, neglecting the nuclear potential diffractive effects. These trajectories present a single turning point. The corresponding fusion cross section is shown in Fig. 3 as a thin line with solid circles. This figure also depicts the full quantum mechanical results (thick solid line). We see that although the approximation obtained with the Rutherford trajectory is reasonable at high energies, it breaks down at energies close and below the Coulomb barrier ( $V_B = 2.67 \text{ MeV}$ ).

The inclusion of the nuclear potential in the trajectory calculations improves considerably the results (thin line with stars). In this case we may have, depending on the partial wave and collision energy, one or three turning points. The treatment with three turning points is not accurate in the region around the Coulomb barrier, and that is the reason why there are large deviations in the approximated fusion cross section. Later we will show how one may improve this approximation, but let us first briefly consider the breakup cross section.

In Ref. [6] the breakup was calculated by considering that

$$T_l^{bu} = 1 - P_l^{surv} . \quad (46)$$

This approximation is based on the notion that  $T_l^{bu}$  corresponds to the probability of non-survival to the breakup process. The results depend strongly on the classical trajectory considered. In Fig. 4 we compare the exact quantum mechanical breakup cross section to the ones obtained using Eq. (46) with different trajectories. The results are far from satisfactory. In particular, when the nuclear potential is included in the trajectory calculations the low energy breakup cross section has a completely wrong behavior. The reason for this discrepancy has been discussed by Takigawa *et al.* [8] and will be considered in further detail later in this section.

Let us now develop an improved WKB approximations for  $T_l^F$  and  $T_l^{bu}$ . In order to explain them, it will be useful to rewrite the  $T_l^F$  coefficients in a different way. In the WKB approximation, the radial wave functions with incoming ( $-$ ) and outgoing ( $+$ ) boundary conditions are given by

$$u_l^{(\pm)}(r) = \frac{A}{\sqrt{k(r)}} \exp \left[ \pm i \int dr k(r) \right] , \quad (47)$$

where

$$k(r) = \frac{1}{\hbar} \sqrt{2\mu \left[ E - U^{opt}(r) - \frac{\hbar^2}{2\mu r^2} l(l+1) - U^{pol}(r) \right]} . \quad (48)$$

The value of  $T_l^F$  is given by the ratio between the probability density current that reaches the strong absorption region,  $j^{(-)}(r = R_F)$ , to the incident one  $j^{(-)}(r = \infty)$ , where the radial currents are

$$j^{(\pm)}(r) = \frac{\hbar}{2\mu i} \left[ \left( u_l^{(\pm)}(r) \right)^* \left( \frac{du_l^{(\pm)}(r)}{dr} \right) - u_l^{(\pm)}(r) \left( \frac{du_l^{(\pm)}(r)}{dr} \right)^* \right] . \quad (49)$$

From Eqs.(47) to (49), we obtain

$$T_l^F = \frac{j^{(-)}(r = R_F)}{j^{(-)}(r = \infty)} \approx \exp \left[ -2\bar{\Phi} \right] , \quad (50)$$

where

$$\bar{\Phi} = \text{Im} \left\{ \int_{R_F}^{\infty} dr k(r) \right\} . \quad (51)$$

If one does not include the polarization potential, the integrand in the equation above is real on the whole classically allowed region (note that  $W^{opt}(r > R_F) = 0$ ). In this way, only the classically forbidden region contributes to attenuate the current that reaches the fusion region ( $r < R_F$ ), *i.e.*

$$\bar{\Phi} \rightarrow \Phi = \int_{r_{in}}^{r_{out}} dr k(r), \quad (52)$$

where  $r_{in}$  and  $r_{out}$  are the inner and outer turning points. In this case  $T_l^F$  reduces to the expression given in Eq. (36).

However, if there is long-ranged absorption as a result of the coupling to the breakup channels, the integrand in Eq. (51) becomes complex in all the integration region. The contributions to the integral that defines  $\bar{\Phi}$  from the classically allowed and forbidden regions may be calculated separately. In this case,  $T_l^F$  is written as the product of factors resulting from each of them. Disregarding the imaginary part of  $U^{pol}(r)$  in the classically forbidden region, the corresponding factor reduces to the WKB tunneling probability  $T_l$ . On the other hand, in the classically allowed regions  $k(r)$  can be calculated in an approximate way. Assuming that the imaginary part of  $U^{pol}(r)$  is small in comparison to the remaining terms in the square root appearing in Eq. (48), we may take a series expansion to the lowest order,

$$k(r) \simeq k_0(r) + i \frac{W^{pol}(r)}{\hbar v(r)}, \quad (53)$$

where

$$k_0(r) = \frac{1}{\hbar} \sqrt{2\mu \left[ E - U^{opt}(r) - \frac{\hbar^2}{2\mu r^2} l(l+1) - V^{pol}(r) \right]} \quad (54)$$

and  $v(r)$  is the local velocity,

$$v(r) = \frac{\hbar k_0(r)}{\mu}. \quad (55)$$

Since  $k_0(r)$  does not attenuate the incident probability current, we obtain the same factor  $P_l^{surv}$  as before.

In our procedure we do not explicitly distinguish between classically allowed and forbidden regions, and calculate  $\bar{\Phi}$  directly from Eq. (51), without any of the additional approximations mentioned in the previous paragraph. In Fig. 5 we show the fusion cross section obtained within this approximation, compared with the exact results and with the old approximation. We see that the present approximation yields excellent results in all energy regions, including the one around the Coulomb barrier where the old approximation totally failed.

As noted by Takigawa *et al.* [8], the relationship between  $T_l^{bu}$  and  $P_l^{surv}$  that appears in Eq. (46) is not actually correct. The reason for this is that when we calculate the survival probability we consider only the incident branch of the trajectory, along which the system approaches the strong absorption region. However, the breakup process may take place both on the entrance or exit branches. Let us first consider the calculation of Ref. [6], which

determines  $P_l^{surv}$  along a Rutherford trajectory. The survival probability associated with  $T_l^{bu}$  is the one calculated along the whole trajectory, *i.e.* along both branches A and B in Fig. 6a, and not just along branch A, as it was done in the calculation of  $P_l^{surv}$ . Since the contribution from both branches to the integral that defines  $\bar{\Phi}$  (Eq. (51)) are equal, the breakup probability amplitude may be written as

$$T_l^{bu} = 1 - (P_l^{surv})^2. \quad (56)$$

If we now take into account the effect of the nuclear potential on the classical trajectory, the situation changes very much. For low partial waves, where  $E > B_l$ , the infinite absorption condition in the strong absorption region allows for only an ingoing branch. On the other side, for partial waves for which  $E < B_l$  we may have two classical turning points, as illustrated in Fig. 6b. In that case all segments A, B, C do contribute to the breakup cross section. In this case the amplitude  $T_l^{bu}$  is given by

$$T_l^{bu} = \frac{[j_l^{(-)}(\infty) - j_l^{(-)}(r_{out})] + [j_l^{(-)}(r_{in}) - j_l^{(-)}(R_F)] + [j_l^{(+)}(r_{out}) - j_l^{(+)}(\infty)]}{j_l^{(-)}(\infty)}. \quad (57)$$

The first term in the numerator corresponds to the contribution to the breakup channel along incoming branch A in Fig. 6b. The second term corresponds to the other incoming segment, C, while the third one is the contribution associated to the exit branch B. The currents in this equation are given by

$$\begin{aligned} j_l^{(-)}(r_{out}) &= e^{-2\Phi_1} j_l^{(-)}(\infty) \\ j_l^{(-)}(r_{in}) &= T_l j_l^{(-)}(r_{out}) \\ j_l^{(-)}(R_F) &= e^{-2\Phi_2} j_l^{(-)}(r_{in}) \\ j_l^{(+)}(r_{out}) &= (1 - T_l) j_l^{(-)}(r_{out}) \\ j_l^{(+)}(\infty) &= e^{-2\Phi_1} j_l^{(+)}(r_{out}), \end{aligned} \quad (58)$$

where  $\Phi_1$  e  $\Phi_2$  are given by

$$\Phi_1 = \text{Im} \left\{ \int_{r_{out}}^{\infty} dr k(r) \right\}; \quad \Phi_2 = \text{Im} \left\{ \int_{r_{in}}^{r_{out}} dr k(r) \right\}. \quad (59)$$

Substituting the density currents in Eq. (57), we obtain

$$T_l^{bu} = [1 - e^{-2\Phi_1}] + e^{-2\Phi_1} [T_l (1 - e^{-2\Phi_2}) + (1 - T_l) (1 - e^{-2\Phi_1})]. \quad (60)$$

The breakup cross section calculated using Eqs. (56) (dashed line) and (60) (full line) are shown in Fig. 7, where they are compared to exact results (solid circles). We notice that the two approximations lead to similar results, and both are reasonably close to the exact values. Comparing the two curves we reach two important conclusions. One is that the inaccuracy in the results in Fig. 4 is due to the omission of the exit branch in the trajectories. The other is that in the present case nuclear effects on the trajectory are not very relevant. This is because the most important contributions to the breakup cross section arise from the high- $l$  partial waves. While for the energy range considered the fusion cross section converges for

$l = 10$ , the breakup one requires the inclusion of partial waves as high as  $l \approx 80$ . In this way, for most partial waves relevant for the breakup calculation the external turning point is placed outside the nuclear potential range. The situation changes somewhat when a more realistic potential is considered. In that case, its intensity decreases at high  $l$  values, and the breakup cross section becomes more sensitive to low partial waves.

#### IV. CONCLUSIONS

We have investigated the validity of commonly used approximations for complete fusion and breakup transmission coefficients in collisions of weakly bound projectiles at near barrier energies. They were tested in the concrete example of the of a  $^{11}\text{Li} + ^{12}\text{C}$  collision. For the calculations, we adopted a typical strong absorption optical potential and, for simplicity, a schematic polarization potential, consistent with theoretical predictions available in the litterature [10,11].

We have shown that the factorization of the complete fusion transmission coefficient as a tunneling factor times a survival probability [2,6–9] may be a reasonable approximation, depending on the classical trajectory used in the evaluation of the latter. However, it is always inaccurate in the neighbourhood of the Coulomb barrier. An improved WKB approximation for  $T_l^F$  was shown to lead to very accurate values of the complete fusion cross section in the whole energy range of our study, both above and below the Coulomb barrier.

We have also shown that the breakup transmission coefficient can be obtained in terms of survival probabilities provided that the emergent branch of the classical trajectory is included in the calculation. However, the accuracy of this approximation is worse than that for complete fusion.

This work was supported in part by CNPq and the MCT/FINEP/CNPq(PRONEX) under contract no. 41.96.0886.00. L.F.C. and R.D. acknowledge partial support from the Fundação Universitária José Bonifácio, and M.S.H. and W.H.Z.C. acknowledge support from the FAPESP.

## REFERENCES

- [1] C.H. Dasso, S. Landowne and A. Winther, Nucl. Phys. A **432** (1985) 495.
- [2] L.F. Canto, R. Donangelo, Lia M. Matos, M.S. Hussein and P. Lotti, Phys. Rev. C **58** (1998) 1107.
- [3] M. Trotta *et al.* Phys. Rev. Letters **84** (2000) 2342.
- [4] J.J. Kolata *et al.* Phys. Rev. Letters **81** (1998) 4580.
- [5] K.E. Rehm *et al.* Phys. Rev. Letters **81** (1998) 3341.
- [6] M.S. Hussein, M.P. Pato, L.F. Canto and R. Donangelo, Phys. Rev. C **46** (1992) 377.
- [7] M.S. Hussein, M.P. Pato, L.F. Canto and R. Donangelo, Phys. Rev. C **47** (1993) 2398.
- [8] N. Takigawa, M. Kuratani and H. Sagawa, Phys. Rev. C **47** (1993) R2470.
- [9] L.F. Canto, R. Donangelo, P. Lotti and M.S. Hussein, Phys. Rev. C **52** (1995) R2848.
- [10] L.F. Canto and R. Donangelo, M.S. Hussein and M.P. Pato, Nucl. Phys. A **542** (1992) 131.
- [11] M.V. Andrés, J. Gómez-Camacho and N.A. Nagarajan, Nucl. Phys. A **579** (1994) 573.
- [12] C.H. Dasso and A. Vitturi, Phys. Rev. C **50** (1994) R12.
- [13] A.M.S. Breitschaft, V.C. Barbosa, L.F. Canto, M.S. Hussein, E.J. Moniz, J. Christley and I.J. Thomson, Ann. of Phys. **243** (1995) 420.
- [14] K. Hagino, A. Vitturi, C.H. Dasso and S. Lenzi, Phys. Rev. C **61** (2000) 037602.
- [15] J. Takahashi *et al.*, Phys. Rev. Letters **78** (1997) 30.
- [16] G.R. Satchler, 'Direct Nuclear Reactions', Oxford University Press, 1983.
- [17] G.R. Satchler, Phys. Rev. C **32** (1985) 2203.
- [18] Herman Feshbach, Ann. Phys. **19** (1962) 287.
- [19] D.L. Hill e J.A. Wheeler, Phys. Rev. **89** (1953) 1102.
- [20] E.C. Kemble, Phys. Rev. **48** (1925) 549.

### Figure Captions

- Figure 1: Hill-Wheeler and WKB approximations to the fusion cross section. The vertical arrow indicates the position of the Coulomb barrier. See text for further details.
- Figure 2: Fusion cross section with different contributions of the polarization potential. See text for details.
- Figure 3: Fusion cross sections obtained with different approximations employed in previous publications. The solid line indicates exact quantum mechanical calculations and the remaining ones are obtained with survival probability approximation (Eq. (44)). The solid circles were obtained with Rutherford trajectories while the stars were obtained with classical trajectories taking into account both the Coulomb and the nuclear potentials.
- Figure 4: Exact breakup cross section (solid line) and cross sections approximated by Eq. (46). The solid circles were obtained with pure Rutherford trajectories while the stars takes into account nuclear potential effects on the trajectory.

- Figure 5: Exact complete fusion cross section (solid circles) compared to the old approximation, depicted also in Fig. 3 (stars), and with the improved WKB approximation (solid line). See text for more details.
- Figure 6: Branches (A, incoming; B, outgoing) of the collision trajectory that contribute to the breakup process, (a) pure Rutherford, and (b) including nuclear potential effects. In this later case, the incoming branch has an additional segment (C).
- Figure 7: Exact calculations of the breakup cross section (solid circles) compared to WKB calculations taking into account all branches of the classical trajectory (A, B, C in Fig. 6b and Eq. (60)) (solid line) and taking only branches A and B in the Rutherford trajectory (Fig. 6a and Eq. (56)) (dashed line).

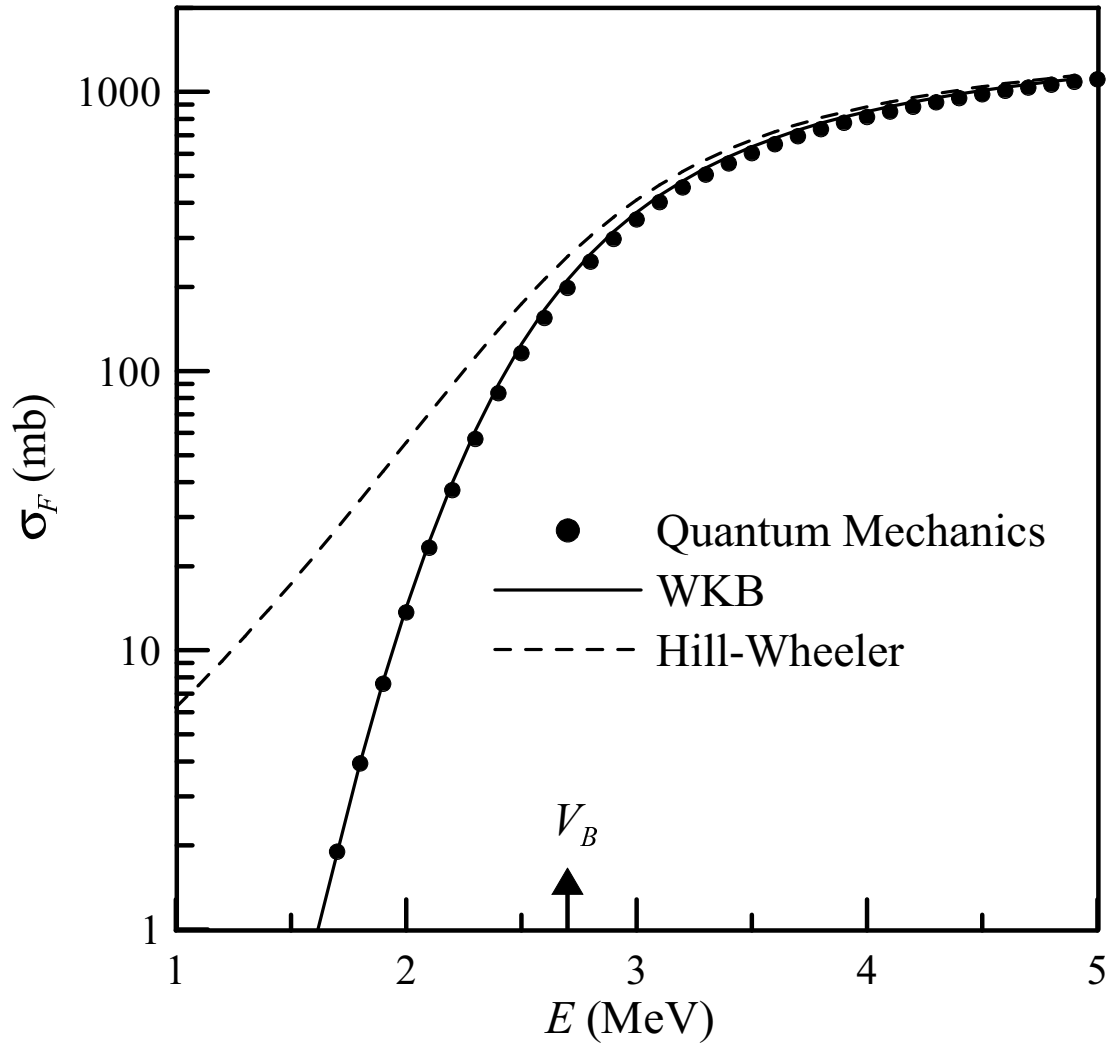


Figure 1



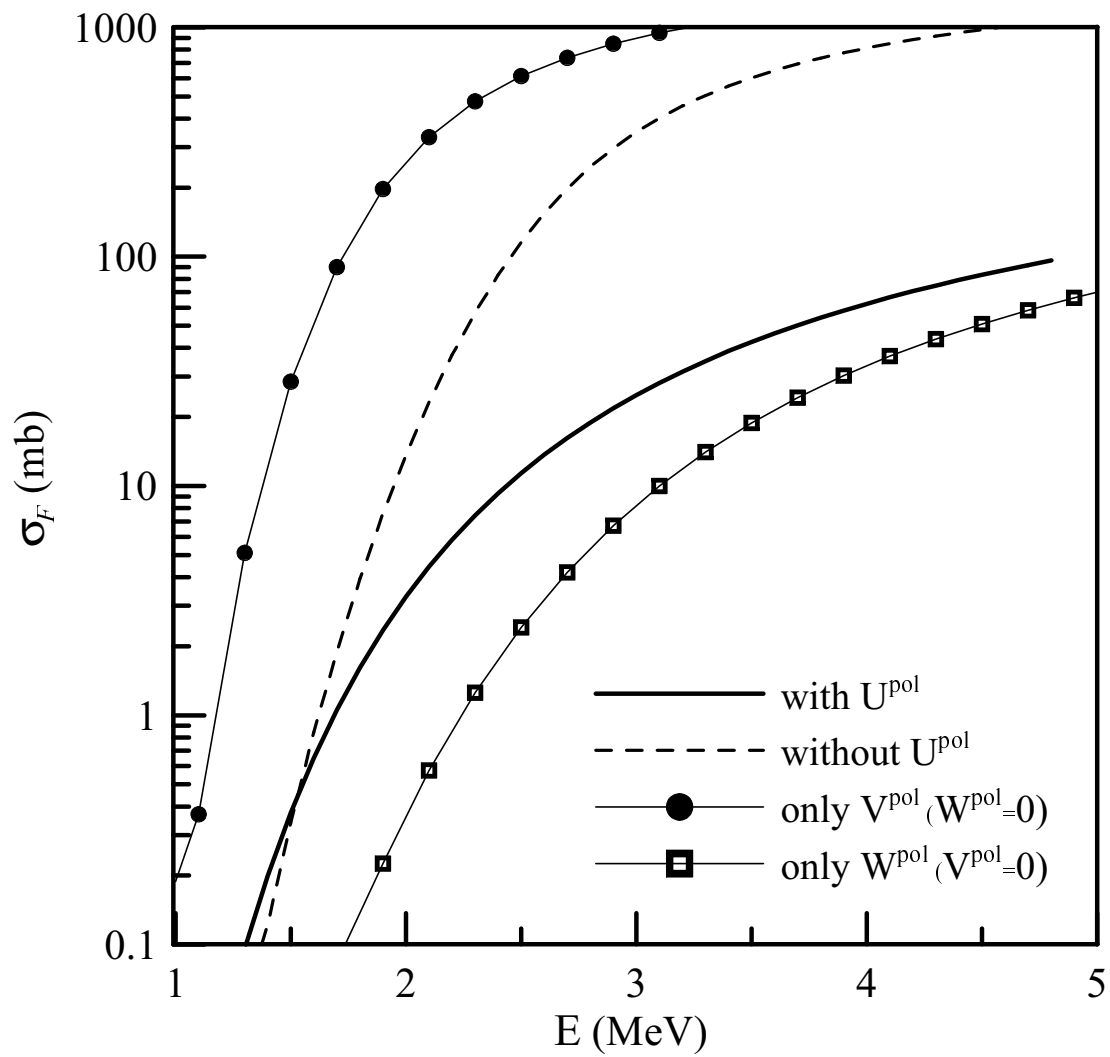


Figure 2

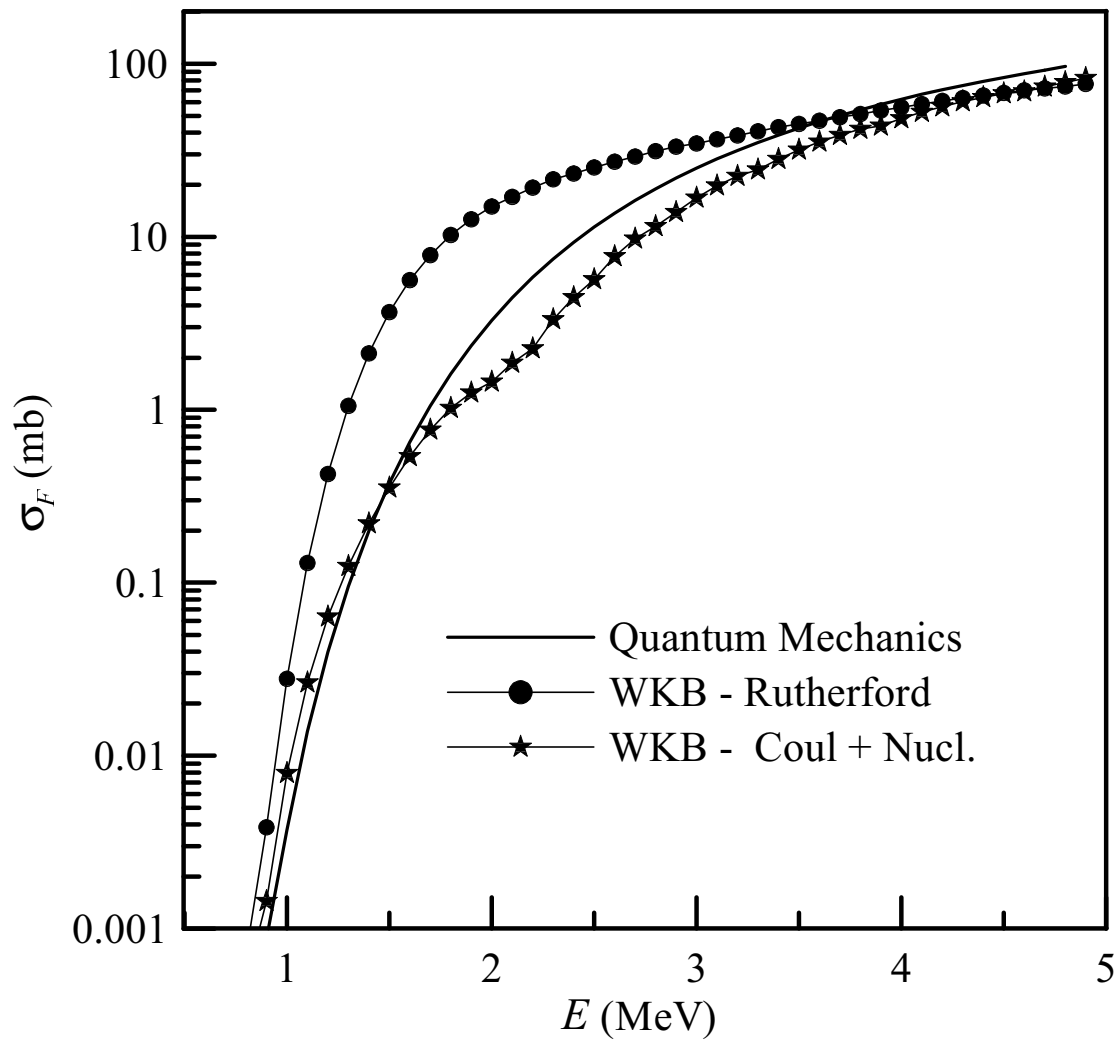


Figure 3

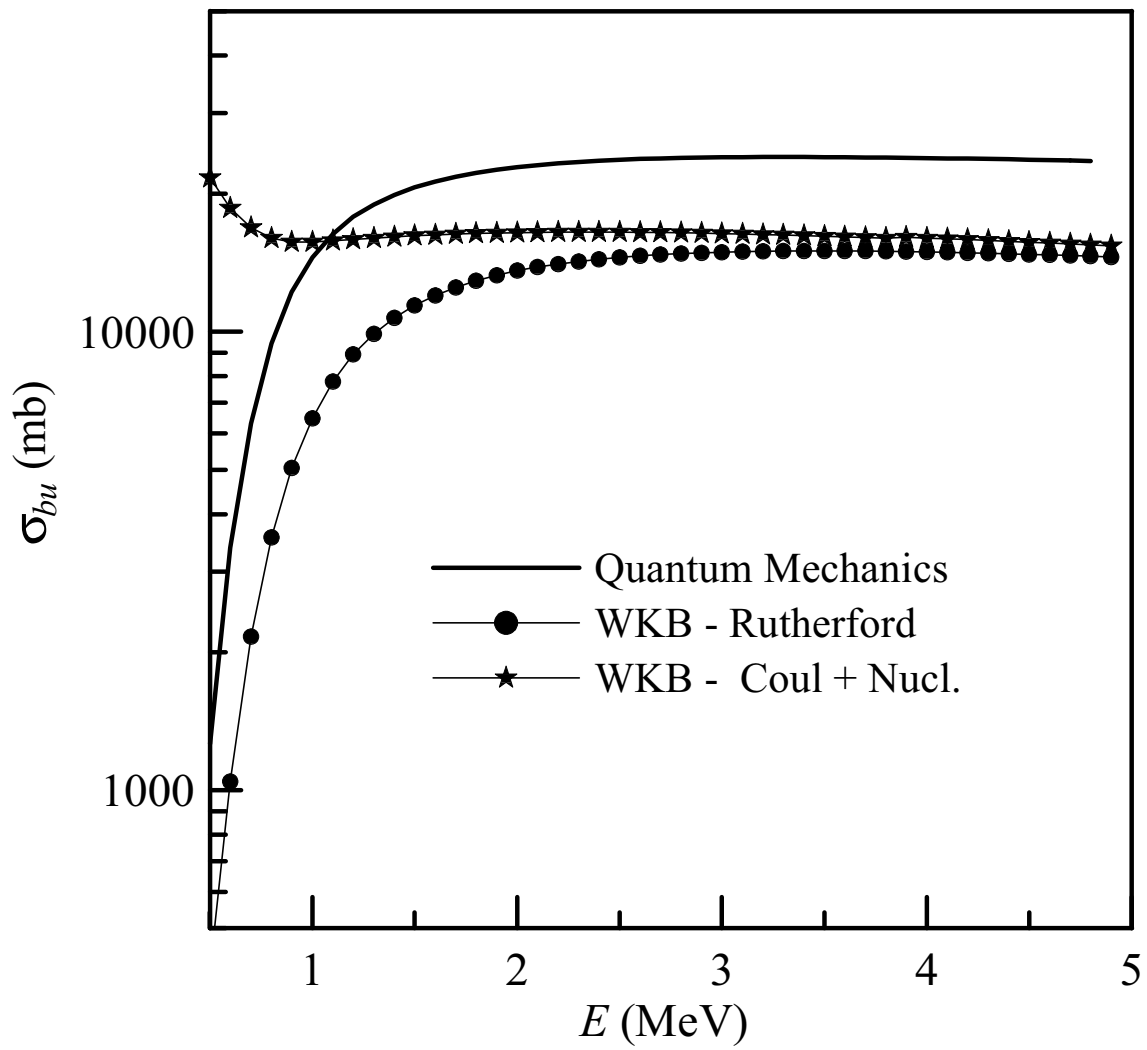


Figure 4

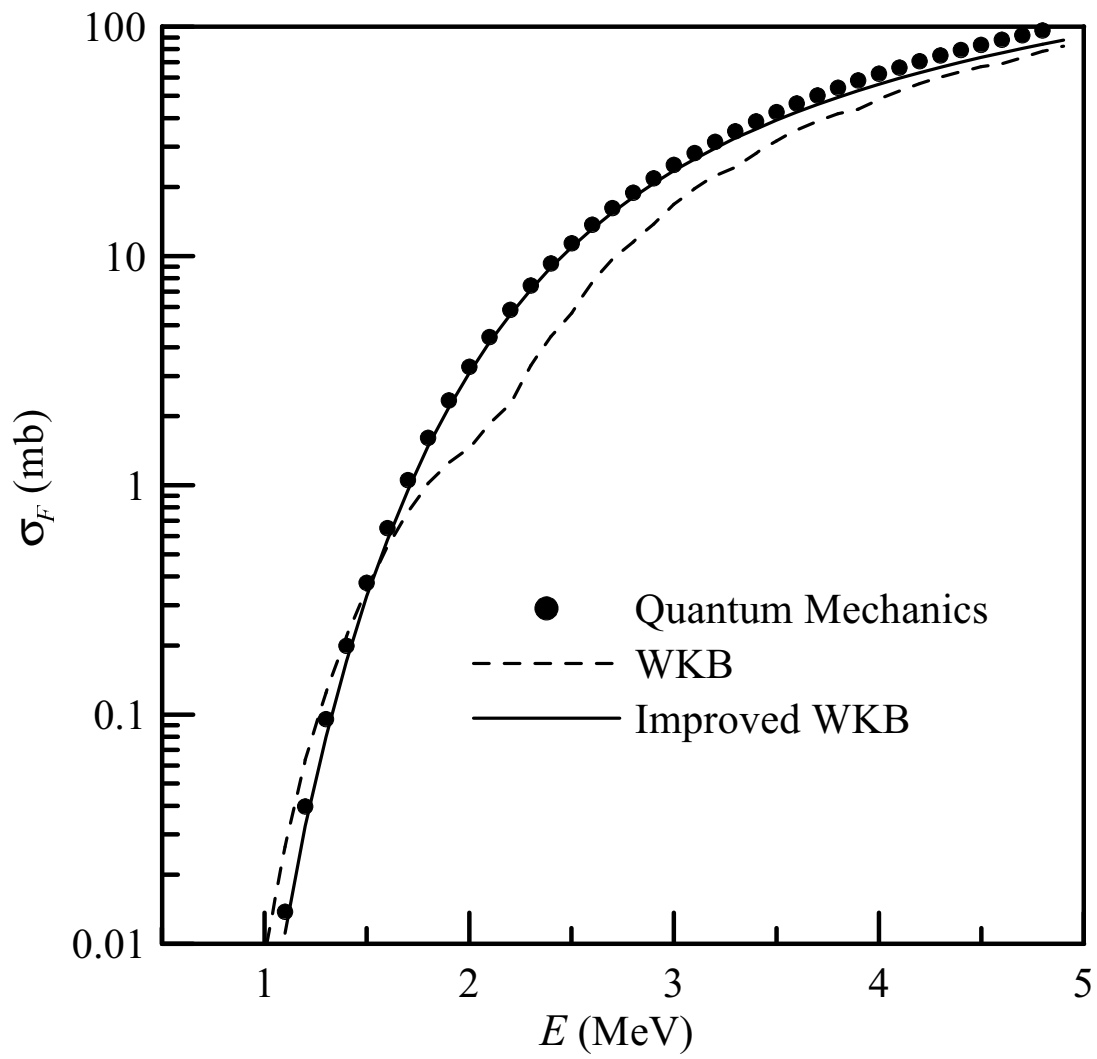
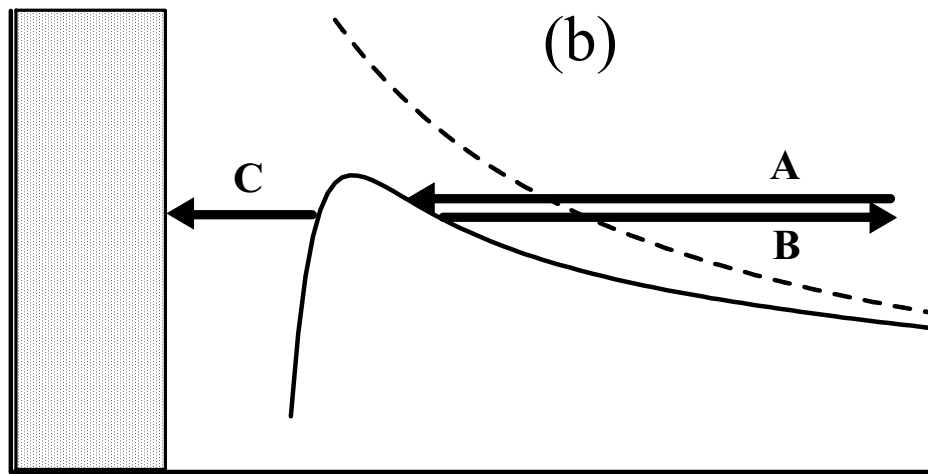


Figure 5



$R_F$

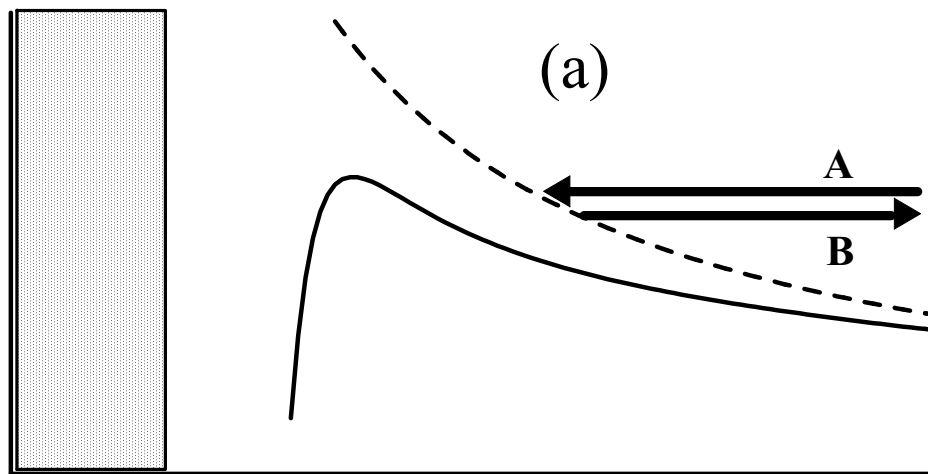


Figure 6

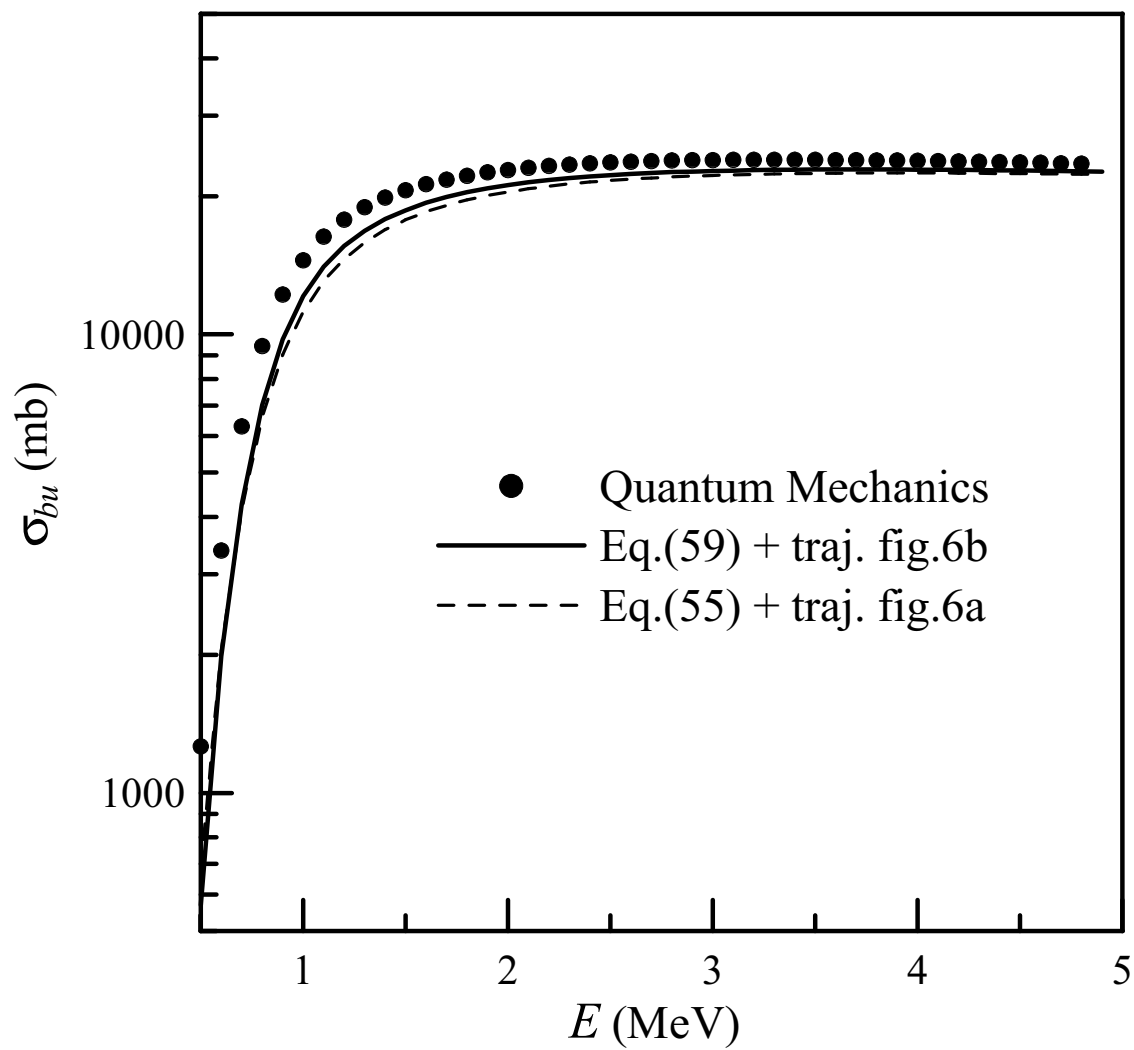


Figure 7